

# Molecular beam epitaxy growth of SiC on Si(111) from silacyclobutane

J. Chen and A. J. Steckl<sup>a)</sup>

*Nanoelectronics Laboratory, University of Cincinnati, Cincinnati, Ohio 45221-0030*

M. J. Loboda

*Dow Corning Corporation, Midland, Michigan 48686-0994*

(Received 5 October 1997; accepted 21 March 1998)

3C-SiC films have been grown by molecular beam epitaxy on Si(111) substrates using a single organosilane precursor (silacyclobutane-SiC<sub>3</sub>H<sub>8</sub>). Temperatures of 800 to 1100 °C and pressures of  $(1-5) \times 10^{-6}$  Torr were utilized. The growth rate of the SiC films obtained from secondary ion mass spectrometry depth profiles ranged from 1 to 6 Å/min. The SiC chemical bonding structure was confirmed by Fourier transform infrared spectrometry. The surface morphology and crystallinity of SiC films were studied by scanning electron microscopy (SEM), reflection high energy electron diffraction and x-ray diffraction. Typical triangular growth pits of various sizes were observed by SEM. X-ray diffraction reveals that SiC films grown in the presence of native oxide exhibit better crystallinity than those grown on surfaces from which the oxide is removed prior to growth. © 1998 American Vacuum Society. [S0734-211X(98)15003-5]

## I. INTRODUCTION

SiC is a wideband gap semiconductor with superior thermal stability and conductivity, high breakdown voltage, and chemical inertness. It is a promising material for high power, high temperature, and high frequency electronic devices. Since SiC substrates are very expensive and their current maximum size is ~2 in., heteroepitaxial growth on Si substrate has become an alternative method for obtaining SiC. Due to the large lattice constant mismatch (20%) and the thermal expansion coefficient difference (8%) between 3C-SiC and Si, considerable effort has been devoted to improving the film quality, leading to a two-step epitaxial growth. The first step is the carbonization of the Si surface by reaction with a hydrocarbon gas to relieve the strain between SiC and Si. This SiC layer is usually too thin (ranging from a few Å's to a few hundred Å's) to fabricate devices. The second step is growth of SiC on the carbonized layer by introducing Si- and C-containing gases. Currently, chemical vapor deposition (CVD) is widely employed to grow epitaxial SiC on Si. SiC CVD growth normally takes place at high temperatures (1200–1350 °C). This can cause deterioration of the film quality and of the SiC-Si interface. Therefore, reduction of growth temperature is an important goal in order to fabricate SiC device with suitable properties.

We have pursued the use of the novel precursor silacyclobutane (SCB-SiC<sub>3</sub>H<sub>8</sub>) as a means to reduce the CVD growth temperature for 3C-SiC on Si<sup>1,2</sup> and on 6H-SiC.<sup>3,4</sup> SCB is a cyclic molecule with one Si atom in a four-member ring. The strained molecular ring is easier to pyrolyze than the alkylsilanes. SCB is a liquid at room temperature with a vapor pressure of ~400 Torr. It is also safer and easier to handle than the common gas system utilized in SiC CVD (such as the silane/propane/hydrogen combination). Films grown by CVD from SCB<sup>2</sup> show that crystalline SiC can be

obtained on Si(111) substrates at growth temperatures as low as 1000 °C without carbonization. Since molecular beam epitaxy (MBE) can provide a very clean growth ambient and better controllability than CVD, MBE growth with SCB could be a promising method to grow high quality SiC films at lower temperatures.

In this article we report the growth of SiC by MBE from SCB on the Si(111) surface and the characterization of these SiC films by secondary ion mass spectrometry (SIMS), Fourier transform infrared (FTIR) absorption spectrometry, scanning electron microscopy (SEM), reflection high energy electron diffraction (RHEED), and x-ray diffraction (XRD). These results are compared to those previously obtained by MBE with the two-step, two-gas method, and also compared to those grown by CVD with SCB in our lab.

## II. EXPERIMENTAL CONDITIONS

The SiC films were grown in a Riber gas source MBE (GSMBE) 32 system. The growth chamber is pumped down to a base pressure of less than  $5 \times 10^{-11}$  Torr by a cryogenic pump with a Ti sublimation pump and extended baking at 200 °C. A quadrupole mass analyzer and a 35 keV RHEED apparatus with an image capture system are mounted on the growth chamber for gas and surface analysis, respectively. The Si substrate is introduced into the growth chamber through a load lock chamber, which is pumped by an ion pump and Ti sublimation pump to a base pressure of  $4 \times 10^{-10}$  Torr.

We have utilized 2 in. (111) Si wafers, boron doped with resistivity of less than 3.5 Ω cm. The wafers were oriented 2°–3° off axis toward (110). They are mounted onto molybdenum blocks with a retaining ring for radiative heating from the rear by a hot Ta filament. The filament current is controlled by a proportional-integral-differential (PID) controller through a thermocouple. The substrate temperature measured by the thermocouple located at the back of the heater is calibrated against a front mounted optical pyrometer, which

<sup>a)</sup>Author to whom correspondence should be addressed; electronic mail: a.steckl@uc.edu

measures the emission from the heated substrate. The SCB purity is  $>99.5\%$ , as determined by gas chromatography and mass spectrometry. SCB is introduced into the growth chamber through a high precision pressure controller. The amount introduced into the growth chamber is monitored by an ion gauge.

The MBE growth process generally consisted of the following steps: (a) loading of the Si wafer into the load lock chamber and transfer to the growth chamber; (b) ramping of substrate temperature to  $700\text{ }^{\circ}\text{C}$  at a rate of  $60\text{ }^{\circ}\text{C}/\text{min}$ ; (c) SCB introduction into the growth chamber at a pressure of  $(1-5)\times 10^{-6}$  Torr, while ramping the temperature to final growth condition at a rate of  $20\text{ }^{\circ}\text{C}/\text{min}$ . Two wafer preparation methods were employed before growth:

- (i) In method I, the Si substrate was only degreased by ultrasonically rinsing in acetone and methanol for 3 min each before introducing it into the growth chamber.
- (ii) In method II, after the degreasing process, the native oxide was removed by dipping the Si substrate in 1% HF for 60 s before loading into the chamber. The sample was further treated by annealing at  $700\text{ }^{\circ}\text{C}$  in ultrahigh vacuum (UHV) until a sharp Si(111) ( $7\times 7$ ) RHEED pattern was obtained.

The composition-depth profile of the SiC films was obtained by SIMS using  $\text{Cs}^+$  bombardment with positive ion detection. Elements monitored during SIMS profiling were C, Si, O, N, and B. Relative sensitivity factors derived from a SiC standard were used to convert ion counts to atomic concentrations. SiC and Si sputtering rates were used to obtain the thickness of the SiC and Si layers, respectively. The chemical bonding of the film constituents was investigated by transmission mode FTIR. An unprocessed Si(111) wafer was used as reference and its FTIR spectrum was subtracted from those taken from SiC/Si(111) samples. The film crystallinity, surface structure, and morphology were characterized by x-ray diffraction, RHEED, and SEM.

### III. RESULTS AND DISCUSSION

The composition of the SiC films was determined by SIMS depth profiling. A typical depth profile of a SiC film on Si(111) is shown in Fig. 1. This film was grown at  $1000\text{ }^{\circ}\text{C}$  and a pressure of  $4.7\times 10^{-6}$  Torr in the presence of native oxide (method I). The film composition of Si and C is fairly uniform for a depth of  $200\text{ }\text{\AA}$ . A long carbon tail into the Si substrate is observed, which could be caused by several effects: (a) absence of an abrupt interface between the SiC film and Si substrate, due to carbon atoms diffusing into the Si during growth or to SiC particles present in the triangle pits which could be more than thousands of  $\text{\AA}$ 's deep; (b) nonuniform film thickness resulting in certain locations where the SiC layer is removed sooner during SIMS profiling. The SIMS data also show that N and B impurities are present in a concentration of less than 0.1% in the SiC film

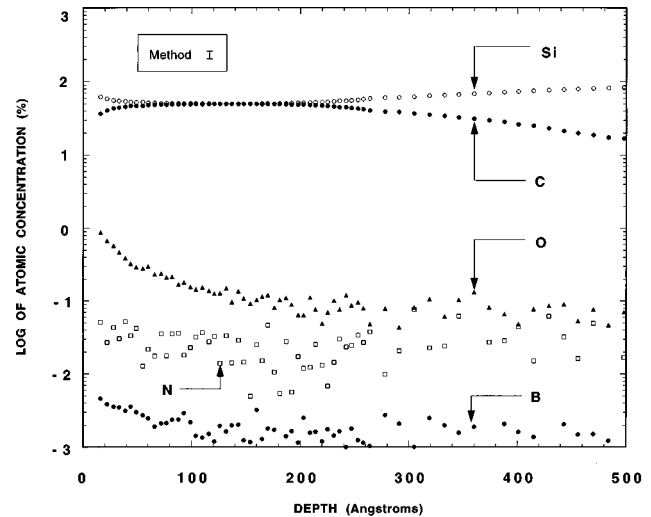


FIG. 1. SIMS depth profile of SiC film grown at  $1000\text{ }^{\circ}\text{C}$  and a pressure of  $4.7\times 10^{-6}$  Torr (method I).

and O concentration is from 1% to 0.1%. The growth rate is  $3.3\text{ }\text{\AA}/\text{min}$ , which is in the range reported for SiC growth rate by GSMBE.<sup>5-8</sup>

The chemical bonding of the MBE-grown SiC films was studied by transmission mode FTIR. Figure 2 presents FTIR spectra of SiC films grown by method I at temperatures from  $800$  to  $1100\text{ }^{\circ}\text{C}$ . Only the Si-C stretching vibration at  $\sim 794\text{ cm}^{-1}$  is observed. The full width at half maximum (FWHM) of the Si-C peaks obtained from SiC films grown at  $800$ ,  $1000$ , and  $1100\text{ }^{\circ}\text{C}$  are  $28$ ,  $23$ , and  $20\text{ cm}^{-1}$ , respectively. These data show that increasing the growth temperature results in a narrower FTIR peak width, indicating improved bonding uniformity within the film. Figure 3 compares the FTIR spectra of SiC films grown by method I and II. These films were grown at  $1000\text{ }^{\circ}\text{C}$  for 80 min. The FTIR peak in the film grown by method II shifts to  $799\text{ cm}^{-1}$  compared to that of the film grown by method I ( $794\text{ cm}^{-1}$ ). The FWHM of the method II film ( $27\text{ cm}^{-1}$ ) is also slightly larger than that of the method I film ( $23\text{ cm}^{-1}$ ). Finally, the intensity of the method II FTIR peak is much smaller than

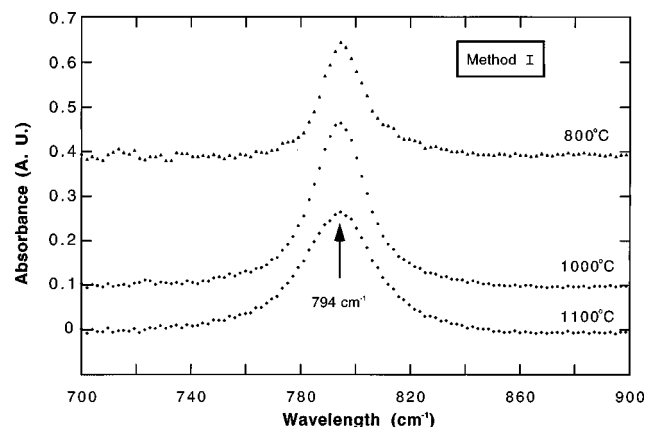


FIG. 2. FTIR spectra of SiC films grown at  $800$ ,  $1000$ , and  $1100\text{ }^{\circ}\text{C}$  (method I).

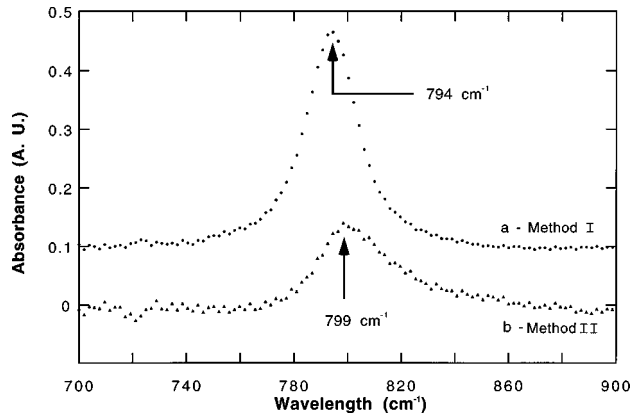


FIG. 3. FTIR spectra of SiC films grown at 1000 °C with (method I) and without (method II) native oxide.

that of the method I film. The FWHM of the Si–C peaks obtained from SiC grown with MBE at 1000 °C by both methods is comparable to that obtained from SiC grown by CVD with SCB<sup>2</sup> at 1200 °C and is about one half of the value obtained for a CVD film grown at 1000 °C. The FWHM of the Si–C FTIR peak reported for SiC films grown by MBE with the two-step, two-gas process<sup>5,9</sup> is similar to the value we have obtained with our one-step, one-gas process.

RHEED patterns from SiC films grown on Si(111) indicate that the SiC crystal orientation follows that (111) substrate. In Fig. 4, we show RHEED images obtained from the SiC surface grown with native oxide (method I) at 800, 1000, and 1100 °C [Figs. 4(a)–4(c)] and from the SiC surface grown without native oxide (method II) at 1000 °C [Fig. 4(d)]. *In situ* RHEED images showed that SiC films start to grow when the substrate temperature reaches ~750 °C. During the transition from Si (1×1) RHEED pattern to SiC RHEED pattern, no obvious diffuse pattern was observed. The RHEED patterns of SiC films prepared with method I and grown between ~750 and ~850 °C are composed of both rings and spots, as seen in Fig. 4(a). At a growth tem-

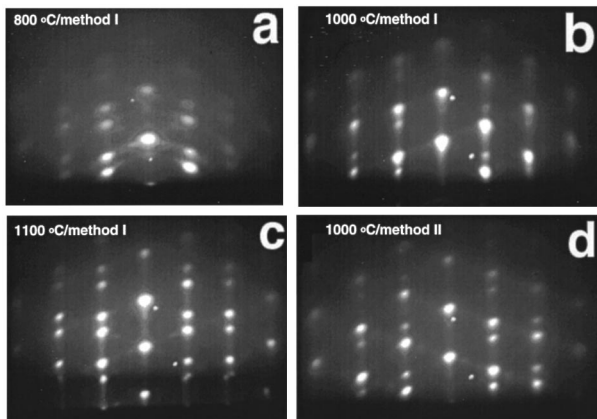


FIG. 4. RHEED images of SiC films grown at: (a) 800 °C—method I; (b) 1000 °C—method I; (c) 1100 °C—method I; (d) 1000 °C—method II. The primary beam is on (110) azimuth.

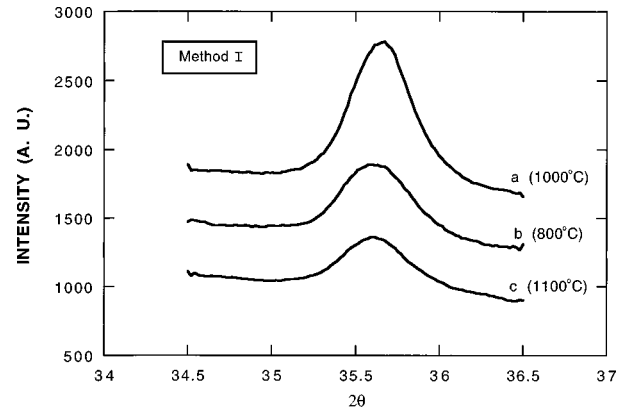


FIG. 5. XRD of SiC films grown with method I at: (a) 1000 °C, for 80 min, FWHM=0.33°; (b) 800 °C, for 55 min, FWHM=0.38°; (c) 1100 °C, for 75 min, FWHM=0.34°. The SCB partial pressure during growth was  $4.7 \times 10^{-6}$  Torr.

perature of 1000 °C and above [Figs. 4(b) and 4(c)], only a spot pattern was observed, which indicates a well-ordered SiC surface. Interestingly, the RHEED images from SiC films grown on Si(111) with method I are not distinguishable from those grown on Si(111) with method II. For example, Fig. 4(d) is a RHEED image of SiC grown at 1000 °C without oxide (method II), while Fig. 4(b) contains the RHEED pattern from the SiC surface grown under the same conditions except for the presence of the native oxide (method I). The spotty patterns appear essentially identical and indicate the same condition of surface crystallinity. These RHEED images and related surface quality are similar to those of previous reports<sup>10,11</sup> on SiC by MBE which utilized the more complicated two-step method. The twin spots clearly visible in the SiC(111) RHEED pattern are believed to be caused by anti-phase domains.<sup>12</sup>

RHEED can only provide crystallinity information of the top several monolayers of the surface, while XRD can penetrate the entire SiC films. Since the SiC films grown under our conditions are quite thin (<500 Å), we had to utilize conventional  $\theta-2\theta$  x-ray diffraction because rocking curve measurements did not produce sufficient signal for accurate measurements. XRD spectra of the SiC films exhibit a strong

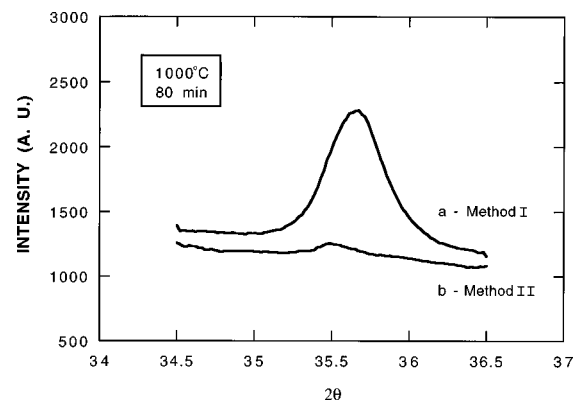


FIG. 6. XRD of SiC films prepared with both method I and II and grown at 1000 °C.

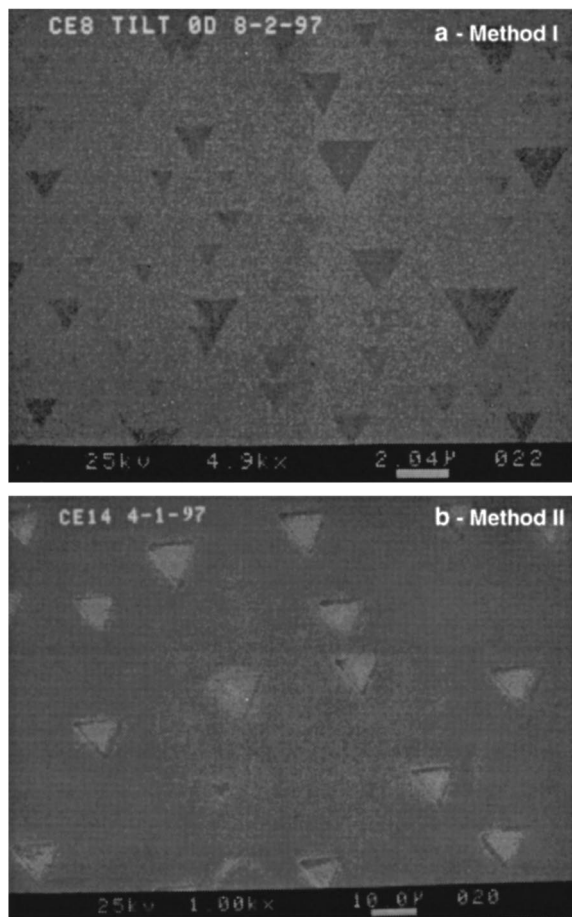


FIG. 7. SEM images of SiC surfaces grown at 1000 °C: (a) with native oxide—method I, image taken at  $\sim 5\text{k}\times$  mag; (b) without native oxide—method II, image taken at  $1\text{k}\times$  mag.

Si(111) peak at  $2\theta = 28.41^\circ$  and a smaller SiC(111) peak at  $\sim 35.7^\circ$ . No peak corresponding to other SiC orientations was observed. This indicates that oriented SiC films were obtained. The films whose XRD spectra are shown in Fig. 5 were prepared by method I and grown at substrate temperatures of 800, 1000, and 1100 °C. The corresponding growth time was 55, 80 and 75 min, respectively. The FWHMs of curve “a-1000 °C” ( $0.33^\circ$ ) and curve “c-1100 °C” ( $0.34^\circ$ ) are smaller than that of curve “b-800 °C” ( $0.38^\circ$ ) of Fig. 5, which indicates that the SiC crystallinity is improved by growing at higher temperatures (1000 and 1100 °C) than at lower temperatures (800 °C). This is consistent with RHEED observations. The FWHMs of curves *a* and *c* are also smaller than those reported from SiC films grown by MBE with the two-step, two-gas process under various conditions.<sup>5,6,9</sup> Figure 6 compares the XRD spectra of SiC films prepared with both method I and method II. These films were grown at 1000 °C for 80 min. The peak in curve *b* (without native oxide-method II) of Fig. 6 is much smaller and broader than that in curve *a* (with native oxide-method I), which indicates that the SiC crystallinity is significantly affected by the presence of the native oxide. This observation is similar to those reported for SiC MBE with  $\text{C}_2\text{H}_2$  on

Si.<sup>13,14</sup> Possible explanations for this phenomenon include: (1) the existence of oxide can moderate the reaction rate during the nucleation phase and therefore prevent (or reduce) the out-diffusion and thermal surface etching of Si; (2) the thicker SiC films grown with oxide present, as indicated by FTIR and SIMS depth profiling, are less affected by the defects generated at the SiC/Si interface due to the 20% lattice mismatch.

The SiC surface was in general quite smooth and uniform. The typical triangular growth pits are observed in the (111) Si substrate. Figure 7 shows SEM images of the SiC films grown at 1000 °C with and without the native oxide. It is interesting to note that the pit size for growth on the “clean” Si(111) surface (method II) is much larger than that for growth with native oxide (method I), while the opposite is true for pit density. For example, in Fig. 7(a), the triangular pits range in size from 1 to 2  $\mu\text{m}$ , whereas the triangular pits shown in Fig. 7(b) range from 5 to 10  $\mu\text{m}$ . This observation indicates that the presence of oxide increases the number of nucleation sites and accelerates the pit seal-off process during the initial stages of the SiC growth.

#### IV. SUMMARY

In summary, RHEED, XRD, SIMS, FTIR, and SEM were employed to characterize SiC films MBE grown from SCB. One-step growth of SiC layers on Si from a single gas precursor at low temperatures by MBE method is proven possible. To our knowledge, this is the first report on the growth of SiC by GSMBE with SCB and the first time SiC has been grown by GSMBE without carbonization. The presence of a native oxide was shown to play a critical role in the growth of crystalline SiC films.

#### ACKNOWLEDGMENTS

The authors are pleased to acknowledge the current support of this work by BMDO/ARO (L. Lome and J. Zavada). Equipment support was provided by grants from the Ohio Materials Network and from the ARO URI program.

- <sup>1</sup>A. J. Steckl, C. Yuan, J. P. Li, and M. J. Loboda, *Appl. Phys. Lett.* **63**, 3347 (1993).
- <sup>2</sup>C. Yuan, A. J. Steckl, and M. J. Loboda, *Appl. Phys. Lett.* **64**, 22 (1994).
- <sup>3</sup>C. Yuan, A. J. Steckl, J. Chaudhari, R. Thokola, and M. J. Loboda, *J. Appl. Phys.* **78**, 1271 (1995).
- <sup>4</sup>J. Chaudhari, X. Chang, C. Yuan, and A. J. Steckl, *Thin Solid Films* **292**, 1 (1997).
- <sup>5</sup>T. Sugii, T. Aoyama, and T. Ito, *J. Electrochem. Soc.* **137**, 989 (1990).
- <sup>6</sup>H. Yamada, *J. Appl. Phys.* **65**, 2084 (1989).
- <sup>7</sup>S. Motoyama, N. Morikawa, M. Nasu, and S. Kaneda, *J. Appl. Phys.* **68**, 101 (1990).
- <sup>8</sup>S. Tanaka, R. S. Fern, and R. F. Davis, *Appl. Phys. Lett.* **65**, 2851 (1994).
- <sup>9</sup>K. Kim, S.-D. Choi, and K. L. Wang, *Thin Solid Films* **225**, 235 (1993).
- <sup>10</sup>S. Motoyama, N. Morikawa, and S. Kaneda, *J. Cryst. Growth* **100**, 615 (1990).
- <sup>11</sup>T. Yoshinobu, H. Mitsui, T. Fuyuki, and H. Matsunami, *J. Appl. Phys.* **72**, 2006 (1992).
- <sup>12</sup>M. Kitabatake, M. Deguchi, and T. Hirao, *J. Appl. Phys.* **74**, 4438 (1993).
- <sup>13</sup>T. Yoshinobu, T. Fukuki, and H. Matsunami, *Jpn. J. Appl. Phys., Part 2* **30**, L1086 (1991).
- <sup>14</sup>T. Yoshinobu, H. Mitsui, Y. Tarui, T. Fukuki, and H. Matsunami, *J. Appl. Phys.* **72**, 2006 (1992).